J | P | S | T

http://jpst.irost.ir

Journal of Particle Science and Technology

IROST

Dynamic modelling of hardness changes of aluminium nanostructure during mechanical ball milling process

Vahid Bidarian[1,*], Esmaeil Koohestanian[2], Maryam Omidvar[3]

[1] *Young Researchers and Elite Club, Quchan Branch, Islamic Azad University, Quchan, Iran*

[2] *Department of Chemical Engineering, University of Sistan and Baluchestan, Zahedan, Iran*

[3] *Department of Chemical Engineering, Quchan Branch, Islamic Azad University, Quchan, Iran*

HIGHLIGHTS

- Elastic and plastic deformation effects during collision were investigated.
- The combination of NFD and powder hardness model shows better results.
- This model is compared to Maurice et.al. The results show a 35% increase in model accuracy.

GRAPHICAL ABSTRACT

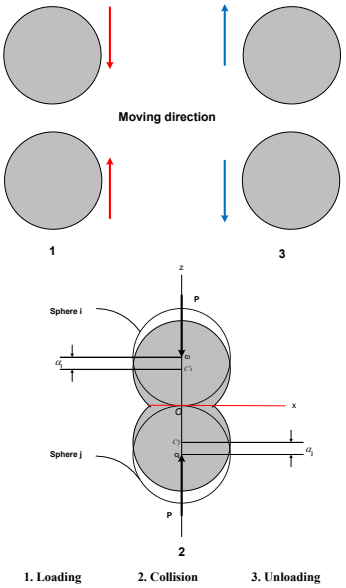

ARTICLE INFO

Article history:
Received 19 August 2016
Revised 4 June 2017
Accepted 11 July 2017

Keywords:
Ball milling
Modelling
Nanostructure
NFD model
Aluminium powder

ABSTRACT

In this research, the feasibility of using mathematical modelling in the ball milling process has been evaluated to verify the hardness changes of an aluminium nanostructure. Considering the model of normal force displacement (NFD), the radius of elastic-plastic and normal displacement of two balls were computed by applying analytical modelling and coding in MATLAB. Properties of balls and aluminium powder were entered into the software as input data. The impact radius and then the hardness of powder were calculated accordingly. The changes of aluminium powder hardness resulting from the collision of two spherical balls during the synthesis of an aluminium nanostructure were analytically derived and compared with experimental data obtained from the literature. Calculation of results accuracy shows the model has a better agreement with the experimental data at the beginning than the results from Maurice et al. (R^2= 0.68 in this model).This research innovation is to combine the NFD model with hardness formulation to calculate final hardness.

* *Corresponding author: Tel.: +98-9155892855 ; Fax: +9851-36144034 ; E-mail address: bidarian.vahid@yahoo.com*

DOI: 10.22104/JPST.2017.1527.1047

1. Introduction

Ball milling (BM) is a technique used to synthesize non-crystallized and non-equilibrium metals. In recent decades, a number of nanostructures have been produced by this method [1-4]. The main mechanism involved in BM is the repetition of the cold welding process and particle refraction, leading to the production of nanostructures over time [5]. As crystal defects (such as dislocations and atomic vacuums) are greatly increased during the sharp collisions of balls and powders, the original powders are crushed several times, leading to nano-scale particles [6]. The BM method enables the accruing of nanoparticles at ambient temperature by accelerating the kinetics of many chemical reactions and changing metallurgical modes [7]. Therefore, many materials and structures in solid state can be produced by this method [8]. The simple single-stage ball mills and relatively low cost process will allow the production of more materials and alloys. In recent years, BM has been widely used to synthesize new magnetic metals such as permanent magnets [9,10], iron oxide and micro powders [11]. In spite of studies on many systems, only some parts of the phenomena involved in the BM process have been understood. Considering most of the studies still take place in the laboratory setting, BM modeling aims to identify the affecting factors in this process and optimize the process of particles production by reducing the number of experiments [12]. These models may be used as instruments of process control.

Many models have been developed by various researchers at different levels of precision for the milling process. Some of these models are based on deformation of solids during particle/particle and particle/ball collisions [14]. For example, Hertz offered some solutions for modeling the elastic contact between loaded spheres [15], and Mindlin et al. subsequently developed this model for elastic-plastic contact [16]. Vu-Quoc demonstrated the deficiency in models based on the theory of elastic collisions by showing the main effect of plastic deformation [17]. He proved that application of these models to stimulate dry again flows in most contacts, included plastic deformation, can lead to inaccurate results. The model of normal force displacement (NFD), as suggested by Walton [18], is based on finite element analysis (FEA) and plastic deformation calculation in which a constant elastic deformation rate is applied during the spheres collision. However, experimental results have shown that this parameter depends on the balls' speed before collision. Therefore, the given model is inconsistent with experimental results [19]. Thornton suggested a NFD model with the calculation of elastic and plastic deformation, producing different rebound coefficients for spheres of different speeds [20]. Maurice et al. presented a comprehensive model for BM [21-23]. This model consists of calculating the forces, tension, hardness, collision time, and other required parameters for the process modeling.

Mio et al. studied the effect of rotating direction and rate of rotating speed of chamber to disk in a planetary ball mill [24]. They demonstrated that collision energy may be increased by increasing the rate of chamber speed to disk speed during the initial stages and then it will be reduced to about the critical speed ratio. They also reported that an effective BM process must be performed at critical speed [24].

In this research, a non-linear NFD model has been used to model the collision of two spherical balls. The balls obtain force from the disk and chamber that are used. The ultimate force on the two balls is determined and the limiting factor of the collision is then calculated. The contact radius and indentation rate of the two balls are calculated by changing the normal force from zero to a calculated value. The hardness changes of the particles and the collision time during the milling process are calculated using these parameters. The limiting factor in each collision is the collision force, and the limiting factor of the process is the final hardness of particles.

2. The model algorithm

The following algorithm is applied to model the process.

1. Enter values of the rotating velocity of disk, chamber and ball radius, radius of the chamber and other constants.
2. Divide each collision by 3000 to calculate the radius and normal displacement, and then divide the loading and unloading forces by 1500.
3. Calculate the elastic radius, plastic radius, elastic-plastic radius and normal displacement using the algorithm given in Figure 1.
4. Calculate powder hardness.
5. Compare the calculated powder hardness from the model to final hardness.

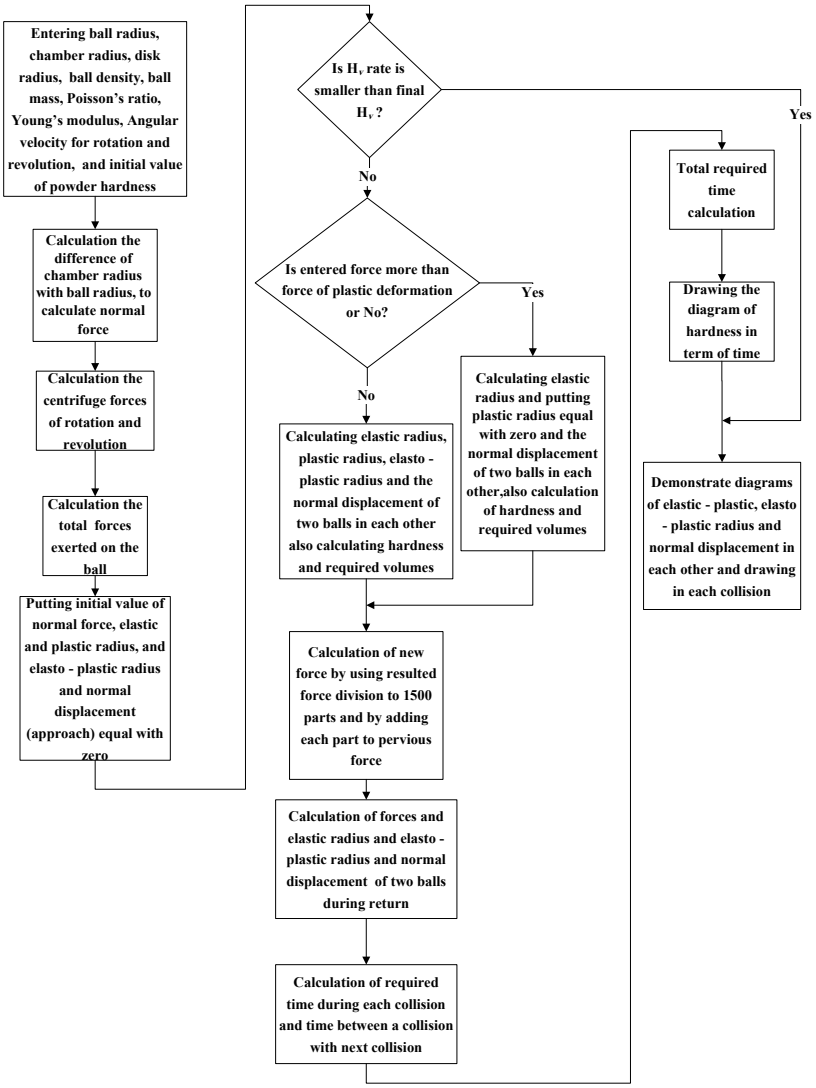

Fig. 1. Box diagram of calculating the powder hardness during BM process.

The mentioned algorithm continues until powder hardness equals the final hardness of the sample. The complete algorithm is shown in Figure 1.

2.1. Calculation of collision force

The total force exerted on the ball is obtained by calculating each force exerted on the ball [24]:

$$F_p = m l_c \omega^2 \quad (1)$$

$$F_r = m(R - l_c)\Omega^2 \quad (2)$$

In the above relations F_p, F_r, and l_c are the centrifugal force of rotation and revolution and l_c is the radius difference of chamber and ball, while ω and Ω are the angular velocity for rotation and revolution.

2.2. Model NFD

According to Figure 2, the kinetic energy of the balls will be converted to deformation energy, while approaching their centers. The energy of deformation is considered as a reduction of distance center to their original center. In order to understand the phenomena, in Figure 2 the real radius of contact has been exaggerated compared to the balls radius.

Corresponding to this energy conversion, tension is considered as the resistance against plastic and elastic deformation. In this model, balls and powder will experience plastic and elastic deformation during collision. In the early stages of contact, powder and balls are deformed elastically, but ultimately deform plastically.

In most collisions, the duration of elastic deformation of powders is shorter than plastic deformation. Thus,

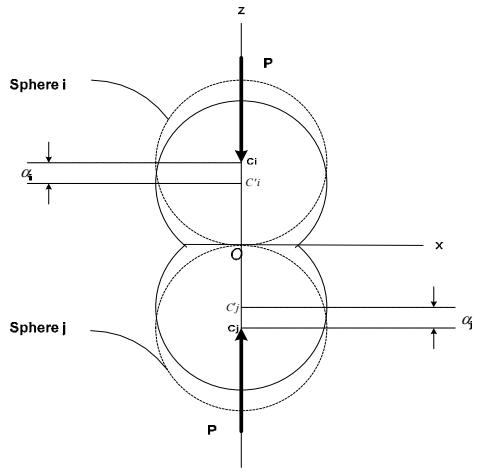

Fig. 2. Two balls contacting with each other and convert kinetic energy to deformation energy during collision of two balls [14].

, the longest-duration collision is considered as plastic deformation. Normal displacement (Figure 2) and deformation can be stated as a function of the radius as follows [22]:

$$a(r) = Rv\left(\frac{\rho_b}{H_v}\right)^{1/2} - \frac{r^2}{R} \tag{3}$$

where r is the distance from center of contact, R is the ball radius, v is the relative velocity of balls during collision, ρ_b is the ball density, and H_v is the powder hardness. The rate of ball normal displacement has been calculated from equation (4):

$$\alpha = \frac{\left(a_{ep}\right)^2}{2R_p^*} \tag{4}$$

In this equation, a_{ep} is the elasto-plastic radius. The equivalent radius of contact area curve (R_p^*) is defined by the following equation [14]:

$$\frac{1}{R_p^*} = \frac{1}{R_{pi}} + \frac{1}{R_{pj}} \tag{5}$$

With regard to the plastic deformation as an irreversible process, (a_{res}) is formed after collision. In order to calculate the normal displacement during the separation of two balls, the following equation is used [14]:

$$a - a_{res} = \frac{\left(a_e\right)^2}{\left(C_R\right)_{p=p_{max}} R} \tag{6}$$

where a_{res} is calculated from Eq. (7) [14]:

$$a_{res} = a_{max} - \frac{\left(a^e\right)_{max}{}^2}{\left(C_R\right)_{(p=p_{max})} R} \tag{7}$$

In this equation, $a^e{}_{max}$ and a_{max} are the normal displacement of maximum force and elastic radius rate, respectively. C_R is the coefficient of radius adjustment to calculate plastic deformation [14]:

$$C_R(p) = \begin{cases} 1 & for\ P \le P_y \\ 1 + K_c\left(P - P_y\right) & for\ P > P_y \end{cases} \tag{8}$$

In the equation above, p_y is the threshold force, in which elastic radius is converted to plastic radius. In the relationship K_c is constant, and is determined according the ball characteristics [14]. Regardless of the type of milling, the BM process is described by collision between powder and milling components; hence, the model of a planetary ball mill has been used. There are several geometric possibilities to treat these collisions. For example, the powder may be trapped among the balls or may end up between ball and milling chamber.

Since the possibility of crushing the powder between the balls is more than that of between the balls and milling chamber [21], this type of collision has been examined in this study. It should be noted that for a different collision (for example a collision between the chamber wall and ball) only the geometric factor is different.

In this model, only crushing and deformation of powder by direct collision has been considered, and other collisions have been neglected. This analysis is used when a little powder covers the balls.

Process parameters and material property data are provided in Tables 1 and 2, respectively.

Table 1. The used parameters in model [23]

Process Parameter	Al (MAP1)
Ball diameter (mm)	6.35
Ball density (g/cm^3)	7.8
Charge ratio	6.3
h_0 (μm)	100
Impact angle (deg)	0
Impact velocity (m/s)	4.0
Impact frequency (s^{-1})	7.28

Figures 3-5 show the NFD curves and related coefficients of restitution generated by our elasto-plastic NFD model. Figure 5 shows the elastic-plastic radius of collision in terms of the normal displacement of two balls into each other during a collision and the return of

Table 2. The physical characteristics of aluminum used in the model [23]

Property	
Modulus (GPa)	72
Tensile strength (MPa)	90
Strain to fracture	0.34
Fracture toughness (MPa$\sqrt{m}$)	20
Density (g/cm)	2.7
Starting hardness (kg/mm^2)	40
Dispersoid diameter (μm)	0.1
Starting particle size (μm)	75
Starting shape factor	0.95
K* (MPa)	104
n*	0.37
Weight fraction	-
Mass ratio of dispersoid	0, 0.01
Dispersoid hardness (kg/mm^2)	550
$\sigma = \sigma_0 + K_\varepsilon^n$, $H_v = 3\sigma$	

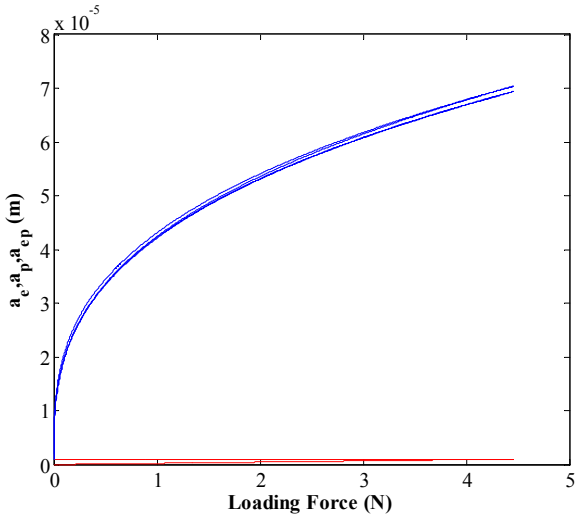

Fig. 3. Elastic, plastic and elastic-plastic radius in term of normal force.

2.3. To change the radius of the contact area

Considering the radius of the contact area from elastic-plastic contact (a_{ep}) and the radius of the elastic contact area (a_e) under force P, the radius of elastic-plastic is determined by Eq. (9):

$$a_{ep} = a_e + a_p \tag{9}$$

$$\begin{cases} a_{ep} = a_e & for\ P \le P_y \\ a_{ep} > a_e & for\ P > P_y \end{cases} \tag{10}$$

Figure 4 shows the radius of plastic contact a_p versus the normal force P for loading and unloading to calculate

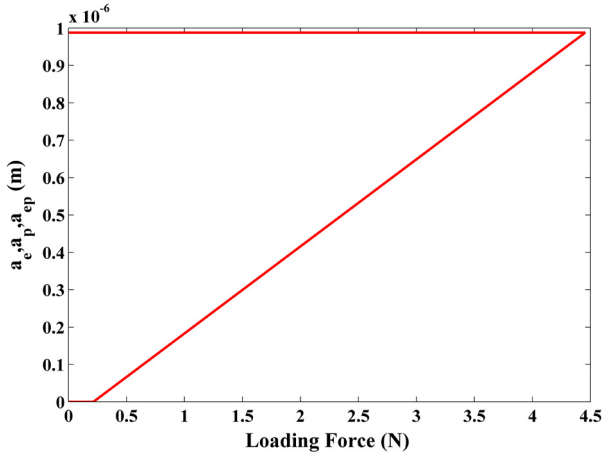

Fig. 4. plastic contact radius in terms of normal contact force.

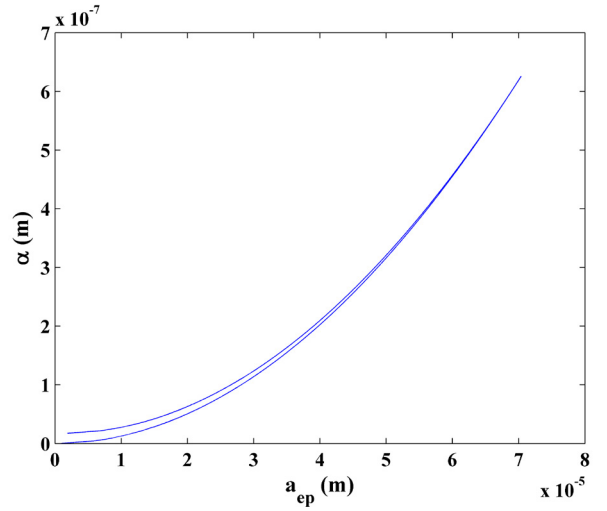

Fig. 5. Normal displacement versus elastic-plastic radius of collision.

calculate the ultimate force from the equation proposed by Mio et al. [24]. It is observed that during loading, plastic radius a_p is increased linearly by increasing force. However, during unloading, the radius of plastic contact a_p is not reduced by reducing P after complete unloading. Stable deformation remains. In other words, when normal force P goes to zero, the contact radius is inclined to non–zero values. Based on these observations, the area of plastic contact a_p is roughly estimated in the proposed model NFD to be as follows [14]:

$$a_P = \begin{cases} C_a\left(P - P_y\right) & for\ loading \\ C_a\left(P_{max} - P_y\right) & for\ unloading \end{cases} \tag{11}$$

C_a is a constant determined according to the characteristics of the contacting balls.

2.4. The collision frequency characteristic

The results of research conducted on distinct collisions

are suitable to determine the collision frequency, and this factor clearly influences the required time to perform the process. The volume of powder with the balls is calculated by the following equation [22]:

$$V_p = \frac{4\pi}{3}\left(\frac{R_b^3 \rho_B}{\rho_p CR}\right) \tag{12}$$

and the powder volume affected by a collision are achieved from Eq. (13):

$$V_c = \pi f_p h_0 a_p^2 \tag{13}$$

where R_b is the ball radius, ρ_b the ball density, CR the charge ratio (mass of balls/mass of powder), ρ_p the powder density, f_p is the volumetric packing factor (typically = 0.6 to 0.7), h_0 the powder thickness coating the balls, and a_p the radius of the plastic contact zone.

The powder volume affected by a collision (V_c, Eq. (13) [4]) is only a small fraction of the powder "associated" with a ball, so it will take several impacts by a given ball before all particles associated with it have been struck once. The number of impacts required for each particle to be struck once (on the average) is given by V_p/V_c, where V_p is the volume of powder associated with each ball:

$$\frac{V_p}{V_c} = \frac{4}{\sqrt{3}}\left(\frac{R_b \rho_b^{(1/2)} H_v^{(1/2)}}{\rho_p CR h_0 v}\right) \tag{14}$$

The time between collisions is obtained using the following equation [21]:

$$\tau = \frac{\pi}{2k} \tag{15}$$

In above equation, coefficient k is calculated as follows [21]:

$$k = \frac{1}{2R}\left[\frac{3H_v}{\rho\left(1+3C^2 tan^2\theta_i\right)}\right]^{1/2} \tag{16}$$

Due to the force angle (θ=0) in this research, the equation is simplified as follows:

$$k = \frac{1}{2R}\left[\frac{3H_v}{\rho}\right]^{1/2} \tag{17}$$

Finally, the duration of collision is calculated from Eq. (18):

$$T = \left(\frac{1}{60\left(\frac{1}{\tau}\right)}\right)\frac{V_P}{V_C} \tag{18}$$

where $1/\tau$ is the impact frequency. Time of each collision is the sum the of τ and T.

2.5. Powder hardness

Hardness is defined as the resistance of a solid material against the penetration of another harder material into its surface. This definition is not completely fulfilled by the usual hardness test methods for metallic materials as shown in Brinell, Vickers and Rockwell. This is due to the fact that the relevant measuring values for the calculation of hardness are measured after removal of test force. Depth sensing indentation gives the possibility to simultaneously record the acting force and corresponding penetration depth [25].

An important process parameter is powder hardness, in which the degree of powder is affected during impact and the normal elastic force acting is determined to separate particles during welding. There is a lack of structural relationship for metals in the strain range which is considered during BM. Thus, a simple plastic structural equation used in the range of less strain will be applied [21], where k is the tenacity coefficient, n is the hardness rate, σ_y is the tension of flow in dense plastic strain and σ_{y_0} is the initial flow. By using $H_v=3\sigma_y$, the following equation is used to determine strain:

$$\sigma_y = \sigma_{y0} + k\varepsilon^n \tag{19}$$

and the equation below is used for strain rate [21]:

$$H_v = H_{v0} + 3k\varepsilon^n \tag{20}$$

$$\varepsilon = -\ln\left(\frac{h_0 - a(r)}{h_0}\right) \tag{21}$$

where $a(r)$ is the normal displacement (approach) of two balls from each other and h_o is the thickness of powder coating the ball. In this way, the determination of strain as a function of radius is simple in the collision area.

2.6 Model accuracy

The accuracy of forecasted values depends on how well the model fits your actual data. The value of R-squared represents the degree of fit. An R-squared value of closer to 1 indicates a better fit and more accurate model. To calculate the model accuracy in this

paper we used the R^2 parameter. To calculate the model accuracy in this paper we used the R^2 parameter. The following equation is used to calculate the R^2 value:

$$R^2 = \frac{\sum_{i=0}^{n}(\hat{y}_i - \bar{y}_i)}{\sum_{i=0}^{n}(y_i - \bar{y}_i)} \quad (22)$$

where y_i is an experimental data, $\hat{y}_i$ is a model data, and $\bar{y}_i$ is the mean of experimental data [26,27].

3. Powder hardness evaluation

Hardness caused by collision can be displayed by factoring certain data into the computational methods. Figure 6 shows the hardness as a function of milling time in the experimental and different calculation methods.

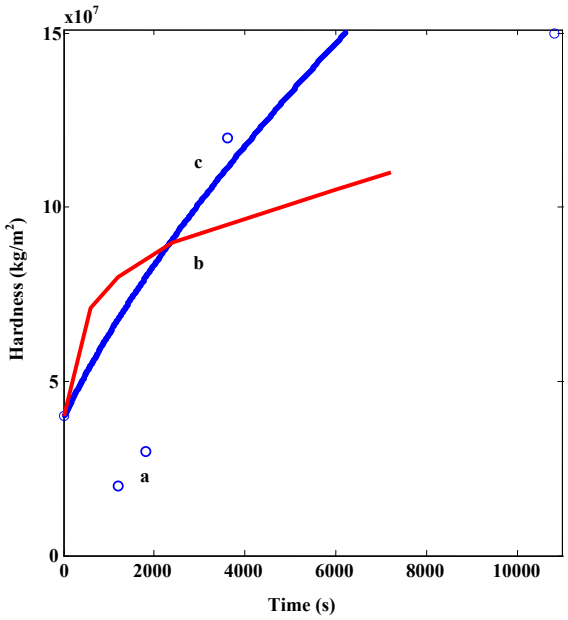

Fig. 6. Hardness changes versus time at ball milling process: a) Experimental data [23], b) Maurice et al. model [23], c) This paper model.

Calculation of results accuracy shows, model has a better agreement with experimental data at the beginning than Maurice et al. By calculating R^2 parameters for the two models (Maurice et al. and this paper), the results show these parameters are 0.5058 and 0.6849, respectively. As a result, the accuracy of our model was 35% more compared to Maurice et al. In this calculation, the point (t =10800, H_v= 150000000) is neglected.

4. Conclusion

Description of aluminum nanostructure hardness represented by a compound model was examined in this study. The two NFD models were combined with the Vo-Quoc model and the given model was used to calculate powder hardness. The results were then compared with the Maurice et al. model and experimental data. In the model developed in this study, the initial properties of powder and ball and its original dimensions were entered into the software. The first condition of collision, the rate of plastic, elastic, and elastic–plastic were then defined. The normal displacement of two balls was calculated by changing the force during the collision. After calculating the indention rate of two balls from the equation, the rate of hardness was calculated. It should be noted that calculation process time was divided in two parts during the collision and time distance between each collision. This was also used in each collision calculation and for numerical values in the model after calculating final hardness. It was observed that the compound model is more compatible with experimental results as compared to the model of Maurice et al. On the other hand, considering the plastic radius, in addition to the elastic radius, the collision will have better compatibility with the experimental data.

Acknowledgments

The authors are grateful to the Research Council of the Quchan Islamic Azad University for financial support of this research.

References

[1] M. Sopicka-Lizer, High-energy ball milling: Mechanochemical processing of nanopowders, Woodhead, New York, 2010.

[2] A. Nazari, M. Zakeri, Modeling the mean grain size of synthesized nanopowders produced by mechanical alloying, Ceram. Int. 39 (2013) 1587-1596.

[3] B. Nasiri-Tabrizi, A. Fahami, R. Ebrahimi-Kahrizsangi, J. Ind. Eng. Chem. 20 (2014) 245-258.

[4] M. Abdellahi, M. Bahmanpour, A novel technology for minimizing the synthesis time of nanostructured powders in planetary mills, Mater. Res. 17 (2014) 781-791.

[5] M.S. Khoshkhoo, S. Scudino, T. Gemming, J. Thomas, J. Freudenberger, M. Zehetbauer, C. Koch, , J. Eckert, Nanostructure formation mechanism

during in-situ consolidation of copper by room temperature ball milling, Mater. Desgin 65 (2015) 1083-1090.

[6] J.S. Benjamin, Mechanical alloying-A perspective, Metal Powder Report. 45 (1990) 122-127.

[7] M.S. El-Asfoury, M.N. Nasr, A. Abdel-Moneim, Effect of Friction on Material Mechanical Behaviour in Non-equal Channel Multi Angular Extrusion (NECMAE), in Book of Abstracts, 2015, pp. 364.

[8] T.P. Yadav, R.M. Yadav, D.P. Singh, Mechanical Milling: a Top Down Approach for the Synthesis of Nanomaterials and Nanocomposites, Nanosci. Nanotech. 2 (2012) 22-48.

[9] M. Zandrahimi, M.D. Chermahini, M. Mirbeik, The effect of multi-step milling and annealing treatments on microstructure and magnetic properties ofnanostructured Fe-Si powders, J. Mag. Mag. Mater. 323 (2011) 669-674.

[10] J. Ding, P. McCormick, R. Street, Structure and magnetic properties of mechanically alloyed SmxFe100-x nitride, J. Alloy. Compd. 189 (1992) 83-86.

[11] J. Ding, W.F. Miao, P.G. McCormick, R. Street, Mechanochemical synthesis of ultrafine Fe powder, Appl. Phys. lett. 67 (1995) 3804-3806.

[12] M. Abdellahi, H. Bahmanpour, M. Bahmanpour, The best conditions forminimizing the synthesis time of nanocomposites during high energy ball milling: Modeling and optimizing, Ceram. Int. 40 (2014) 9675-9692.

[13] A. Canakci, S. Ozsahin, T. Varol, Modeling the influence of a process control agent on the properties of metal matrix composite powders using artificial neural networks, Powder Technol. 228 (2012) 26-35.

[14] L. Vu-Quoc, X. Zhang, L. Lesburg, A normal force-displacement model for contacting spheres accounting for plastic deformation force-driven formulation, J. Appl. Mech. 67 (2000) 363-371.

[15] H. Hertz, Uber die Beruhrung fester elastische Korper and uber die Harts (On the contact of rigid elastic solids and on hardness), Verhandlunger des Vereins zur Beforderung des Gewerbefleisses, Leipzig, Nov. 1882.

[16] R.D. Mindlin, H. Deresiewica, Elastic spheres in contact under varying oblique forces, J. Appl. Mech. 20 (1953) 327-344.

[17] L. Vu-Quoc, X. Zhang, L. Lesburg, Contact force-displacement relations for spherical particles accounting for plastic deformation, Int. J. Solids Struct. 38 (2001) 6455-6490.

[18] O.R. Walton, R.L. Braun, Viscosity, granular-temperature, and stress calculations for shearing assemblies of inelastic, frictional disks, J. Rheol. 30 (1986) 949-980.

[19] W. Goldsmith, Impact, the theory and physical behavior of colliding solids, Edward Arnold Pub., 1960.

[20] C. Thornton, Coefficient of restitution for collinear collisions of elastic-perfectly plastic spheres, J. Appl. Mech. 64 (1997) 383-386.

[21] D. Maurice, T.H. Courtney, Modeling of mechanical alloying: Part I. deformation, coalescence, bdand fragmentation mechanisms, Metall. Mater. Trans. A, 25 (1994) 147–158.

[22] D. Maurice, T.H. Courtney, Modeling of mechanical alloying: Part II. development of computational modeling programs, Metall. Mater. Trans. A 26 (1995) 2431-2435.

[23] D. Maurice, T.H. Courtney, Modeling of mechanical alloying: Part III. Applications of computational programs, Metall. Mater. Trans. A 26 (1995) 2437-2444.

[24] H. Mio, J. Kano, F. Saito, K. Kaneko, Effects of rotational direction and rotation-to-revolution speed ratio in planetary ball milling, Mater. Sci. Eng. A 332 (2002) 75-80.

[25] E. Hryha, P. Zubko, E. Dudrova, L. Pešek, S. Bengtsson, An application of universal hardness test to metal powder particles, J. Mater. Process. Tech. 209 (2009) 2377-2385.

[26] J. Walkenbach, Excel 2013 Formulas, John Wiley & Sons Publisher, 2013, pp. 483.

[27] K. Velten, Mathematical Modeling and Simulation: Introduction for Scientists and Engineers, John Wiley & Sons Publisher, 2009, pp. 69.